Dear Author,

Here are the proofs of your article.

- You can submit your corrections **online**, via **e-mail** or by **fax**.
- For **online** submission please insert your corrections in the online correction form. Always indicate the line number to which the correction refers.
- You can also insert your corrections in the proof PDF and **email** the annotated PDF.
- For fax submission, please ensure that your corrections are clearly legible. Use a fine black pen and write the correction in the margin, not too close to the edge of the page.
- Remember to note the **journal title**, **article number**, and **your name** when sending your response via e-mail or fax.
- **Check** the metadata sheet to make sure that the header information, especially author names and the corresponding affiliations are correctly shown.
- **Check** the questions that may have arisen during copy editing and insert your answers/ corrections.
- **Check** that the text is complete and that all figures, tables and their legends are included. Also check the accuracy of special characters, equations, and electronic supplementary material if applicable. If necessary refer to the *Edited manuscript*.
- The publication of inaccurate data such as dosages and units can have serious consequences. Please take particular care that all such details are correct.
- Please **do not** make changes that involve only matters of style. We have generally introduced forms that follow the journal's style.
  Substantial changes in content, e.g., new results, corrected values, title and authorship are not allowed without the approval of the responsible editor. In such a case, please contact the Editorial Office and return his/her consent together with the proof.
- If we do not receive your corrections **within 48 hours**, we will send you a reminder.
- Your article will be published **Online First** approximately one week after receipt of your corrected proofs. This is the **official first publication** citable with the DOI. **Further changes are, therefore, not possible.**
- The **printed version** will follow in a forthcoming issue.

Please note

After online publication, subscribers (personal/institutional) to this journal will have access to the complete article via the DOI using the URL: http://dx.doi.org/[DOI].
If you would like to know when your article has been published online, take advantage of our free alert service. For registration and further information go to: http://www.link.springer.com.

Due to the electronic nature of the procedure, the manuscript and the original figures will only be returned to you on special request. When you return your corrections, please inform us if you would like to have these documents returned.

Metadata of the article that will be visualized in OnlineFirst

Please note: Images will appear in color online but will be printed in black and white.

ArticleTitle	Lithium Ion Secondary Cell Prepared by a Printing Procedure, and Its Application to All-Solid-State Inorganic Lithium Ion Cells
Article Sub-Title	
Article CopyRight	TMS (This will be the copyright line in the final PDF)
Journal Name	Journal of Electronic Materials

Corresponding Author	Family Name	**Mori**
	Particle	
	Given Name	**Ryohei**
	Suffix	
	Division	
	Organization	Fuji Pigment Co. Ltd.
	Address	2-23-2 Obana, 666-0015, Kawanishi, Hyogo Prefecture, Japan
	Email	moriryohei@fuji-pigment.co.jp

	Received	12 February 2013
Schedule	Revised	
	Accepted	15 January 2014

Abstract

We have developed a straightforward printing method for preparation of a lithium secondary cell. $LiCo_{1/3}Ni_{1/3}Mn_{1/3}O_2$ and $Li_4Ti_5O_{12}$ viscous printable pastes were used for the cathode and anode, respectively. Electrochemical measurement was used to characterize the capacitance of each cell, and field-emission scanning electron microscopy and particle size measurements were used to characterize particle size and morphology. These film electrodes functioned stably both in a standard liquid electrolyte and in an Li_2SiO_3 solid electrolyte, although the capacitance of the all-solid-state cell was significantly lower than that of the cell containing liquid electrolyte. When liquid electrolyte was used, the capacity decreased by 36% after 50 cycles. However, the capacity of 0.2 mA h/g remained almost the same even after 50 charge–discharge cycles, demonstrating the stability and strength of the all-solid-state lithium ion cell. It was also found that the cell resistance mostly arose from the electrode/electrolyte interface and not from the bulk electrolyte. Addition of a sol–gel to the solid electrolyte printable paste improved cell performance.

Keywords (separated by '-') Lithium ion cell - all-solid-state - sol–gel - thin film

Footnote Information

Journal: 11664
Article: 3039

Springer
the language of science

Author Query Form

Please ensure you fill out your response to the queries raised below and return this form along with your corrections

Dear Author

During the process of typesetting your article, the following queries have arisen. Please check your typeset proof carefully against the queries listed below and mark the necessary changes either directly on the proof/online grid or in the 'Author's response' area provided below

Query	Details required	Author's response
1.	Please check and confirm the usage of term squige versus squidge.	
2.	In the sentence "Although the choice of electrolyte... electrode/electrolyte material." we have deleted "and morphology of the electrode/electrolyte material" because this seemed to be repetition. Please check.	
3.	The caption of Figure 5 does not seem to agree with the figure. There are, for example, no insets. Please check.	
4.	Please check the text "as explained at Fig. 5 section". Figure 5 does not seem appropriate for "ion-conductive inorganic glue" (and, in fact, glue has not been discussed elsewhere in the manuscript).	

Journal of ELECTRONIC MATERIALS
DOI: 10.1007/s11664-014-3039-z

Lithium Ion Secondary Cell Prepared by a Printing Procedure, and Its Application to All-Solid-State Inorganic Lithium Ion Cells

RYOHEI MORI[1,2]

1.—Fuji Pigment Co. Ltd., 2-23-2 Obana, Kawanishi, Hyogo Prefecture 666-0015, Japan.
2.—e-mail: moriryohei@fuji-pigment.co.jp

We have developed a straightforward printing method for preparation of a lithium secondary cell. $LiCo_{1/3}Ni_{1/3}Mn_{1/3}O_2$ and $Li_4Ti_5O_{12}$ viscous printable pastes were used for the cathode and anode, respectively. Electrochemical measurement was used to characterize the capacitance of each cell, and field-emission scanning electron microscopy and particle size measurements were used to characterize particle size and morphology. These film electrodes functioned stably both in a standard liquid electrolyte and in an Li_2SiO_3 solid electrolyte, although the capacitance of the all-solid-state cell was significantly lower than that of the cell containing liquid electrolyte. When liquid electrolyte was used, the capacity decreased by 36% after 50 cycles. However, the capacity of 0.2 mA h/g remained almost the same even after 50 charge–discharge cycles, demonstrating the stability and strength of the all-solid-state lithium ion cell. It was also found that the cell resistance mostly arose from the electrode/electrolyte interface and not from the bulk electrolyte. Addition of a sol–gel to the solid electrolyte printable paste improved cell performance.

Key words: Lithium ion cell, all-solid-state, sol–gel, thin film

INTRODUCTION

Lithium ion cells are widely used as power sources for a variety of mobile electronic devices.[1–3] In recent years, the demand for large lithium ion cells for use in electric vehicles (EVs), hybrid electric vehicles (HEVs) in particular, has grown substantially, necessitating improvements in the safety of lithium ion cells. Current commercially-available cells use primarily liquid electrolytes containing organic solvent, which limit the safety and reliability of the cells. Exchanging the flammable liquid electrolytes for non-flammable solid electrolytes has been shown to drastically improve the performance and robustness of lithium ion cells, and all-solid-state lithium secondary cells are expected to be the preferred design for use in EVs and HEVs.

As a result of this high demand, several approaches to preparing all-solid-state cells have been developed,[4–9] including use of such techniques as radio-frequency (RF) sputtering and laser ablation. Another option is a bulk type cell constructed from solid electrolyte and electrode powder. Polymer electrolytes are also good candidates for use in all-solid-state cells, and have been proved to function well with good stability.[8,9] Among inorganic electrolyte materials, sulfide-based glassy materials are favored as solid electrolytes for bulk-type all-solid-state cells, because of their advantages over crystalline solid electrolytes.[10–12] However, sulfides are unsuitable for practical use because of their instability—they react with ambient moisture and emit hydrogen sulfide.

In this respect, inorganic oxide materials are now regarded as the best candidates for use as solid electrolytes in lithium ion cells, because their stability to air and humidity results in great flexibility in their development for practical uses and implementation in industrial manufacturing processes. Several all-solid-state thin film cells with inorganic electrolytes have already been reported. Lithium phosphorus oxynitride (LiPON) has excellent cycling performance at room temperature.[13,14] Sodium (Na)

(Received February 12, 2013; accepted January 15, 2014)

Table I. Comparison of this study with related studies

Battery type	Refs.
LIB with liquid electrolyte	1–3
All-solid-state LIB (RF sputtering, laser ablation)	4,6,7
All-solid-state LIB (polymer electrolyte)	8,9
All-solid-state LIB (sulfide-based materials)	10–12
All-solid-state LIB (oxide material, LIPON type)	13,14
All-solid-state LIB (oxide material, NASICON type)	15,16
All-solid-state LIB (oxide material, printing preparation)	This study

super ionic conductor (NASICON)-type Li-ion conducting electrolyte consisting of Li_2O–Al_2O_3–SiO_2–P_2O_5–TiO_2 has also received much attention because of its high Li-ion conductivity of 10^{-4}–10^{-3} S cm^{-1} at room temperature.[15,16] Our work and related studies are compared in Table I.

Although the choice of electrolyte material is of great importance, lithium ion cell performance is also affected by electrode and solid electrolyte morphology, including particle size. Controlling particle size and morphology is critical to obtaining high-performance lithium ion cells. One method for controlling particle size is an industrial dispersion procedure, which is particularly effective for inorganic materials. In general, particles tend to form aggregates when mixed with liquid, because of van der Waals forces. However, use of an appropriate chemical which adheres to the surface of the particles can disperse the aggregates into small individual particles, as a result of acid–base interactions or three-dimensional repulsive forces.[17]

In this study, we prepared printable viscous pastes for both electrode and electrolyte to make an all-solid-state lithium ion cell by use of a simple printing procedure. In addition, we investigated the effect on lithium ion cell performance of mixing a sol–gel solution with the solid electrolyte printable paste.

EXPERIMENTAL

Active material for the lithium ion cell cathode ($LiCo_{1/3}Ni_{1/3}Mn_{1/3}O_2$) was purchased from Tanaka Chemical (Fukui, Japan). Lithium titanate ($Li_4Ti_5O_{12}$) was purchased from Ishihara Sangyo (Osaka, Japan). Lithium silicate (Li_2SiO_3) powder, tetraethoxysilane (TEOS), lithium nitrate ($LiNO_3$), phosphoric acid (H_3PO_4), and nitric acid (HNO_3) were purchased from Wako Chemical (Osaka, Japan). Terpineol (α-α-4-trimethyl cyclohex-3-ene-1-methanol) was purchased from Arakawa Chemical Industries (Osaka, Japan). The dispersant polyoxyethylene sorbitan tristearate, was purchased from Kao Corporation (Japan).

The appropriate amount of electrode or solid electrolyte powder was dissolved in terpineol, with polyoxyethylene sorbitan tristearate as dispersant. Ethyl cellulose (MW 20,000; Wako Chemical) was added as binder and to increase the viscosity of the dispersion liquid for the squige printing technique. The viscous pastes for the electrode and electrolyte were made by combining 21 g electrode or solid electrolyte powder with 2 g dispersant and 47 g terpineol. These were then dispersed for 30 min by use of a stirring machine rotating at 3500 rpm. Ethyl cellulose (3 g) was added to 45 g sol slurry and the mixture was then stirred for an additional 30 min at 2000 rpm to completely dissolve the ethyl cellulose.

Tetraethoxysilane (TEOS), $LiNO_3$, H_3PO_4, water, and HNO_3 were combined in the molar ratio 1:7:7:1:0.1 to form a sol–gel phase. To suit the scale of our experiment, we combined 5.2 g TEOS, 12.075 g $LiNO_3$, 17.15 g H_3PO_4, 0.1575 g HNO_3, and 0.45 g water, and mixed them with 50 g ethanol. The mixture was added to the solid electrolyte printable paste before printing in a weight ratio of 1:1 (sol–gel solution-to-printable paste). The resulting viscous paste was deposited on to an aluminium plate substrate by squige printing. The film was heat treated at 600°C for 30 min then cooled to room temperature. For all-solid-state lithium ion cell preparation, $LiCo_{1/3}Ni_{1/3}Mn_{1/3}O_2$ was coated on to an aluminium plate, followed by a coat of Li_2SiO_3 paste, and a final coat of $Li_4Ti_5O_{12}$ paste, with heat treatments at each step. For electrochemical measurements of the lithium ion cell containing liquid electrolyte, an electrolyte composed of 1.25 M $LiClO_4$ in 3:1 *v*/*v* ethylene carbonate–propylene carbonate was used. For all-solid-state lithium ion cell electrochemical measurements, copper adhesive tape was placed on top of the $Li_4Ti_5O_{12}$ layer to create an electrical contact. Cell performance was evaluated galvanostatically by use of a charge and discharge apparatus (SP-150; Bio Logics, France). Cut off potential was determined from 2.2 V to 0 V. Electrochemical impedance spectroscopy was conducted from 1 MHz to 100 mHz with a 10 mV amplitude. All electrochemical measurements were conducted under ambient conditions. To determine morphology, the films were imaged by use of field-emission scanning electron microscopy (FESEM; JSM-6700F; Jeol, Tokyo, Japan). The sizes of the dispersed particles were measured by use of a Microtrac particle-size analyzer (Nanotrac TM 150; Nikkiso, Japan); to perform this measurement, the particle dispersion sample was aspirated from the

Journal : 11664_JEM | Dispatch : 1-2-2014 | Pages : 8
Article No.: 3039 | ☐ LE ☑ CP | ☐ TYPESET ☑ DISK

suspension and quickly injected into a solvent solution. The crystalline phase of the solid electrolyte prepared by use of a sol–gel was evaluated by x-ray diffractometry (XRD; RINT 2500 x-ray diffractometer; Rigaku, Tokyo, Japan) using Cu Kα radiation and operated at 40 kV and 50 mA.

RESULTS AND DISCUSSION

Figure 1 shows the discharge curve for the lithium ion cell made with $LiCo_{1/3}Ni_{1/3}Mn_{1/3}O_2$ and $Li_4Ti_5O_{12}$ thin films prepared by a printing procedure. The current density was measured at a constant rate of 20 μA/cm^2. These materials were chosen for the electrodes because of their stability to air and moisture, meaning that both can be prepared and handled under ambient conditions. In addition, it was not necessary to use a fluoride-containing organic solvent that could emit HF by reaction with the ambient atmosphere, because Li metal was not used as an anode. The differences between the electrochemical properties of $LiCo_{1/3}Ni_{1/3}Mn_{1/3}O_2$ and $Li_4Ti_5O_{12}$ and those of Li metal are well understood.[18–21] For intercalation cells made without any metallic lithium, intermediate voltages were related to the difference between the positive ($LiCo_{1/3}Ni_{1/3}Mn_{1/3}O_2$: 3.6 V) and negative ($Li_4Ti_5O_{12}$: 1.6 V) electrode potentials. The electrochemical charge–discharge curves for $LiCo_{1/3}Ni_{1/3}Mn_{1/3}O_2/Li_4Ti_5O_{12}$ at a current density of 20 μA/cm^2 in EC–PC electrolyte indicated that Li was de-intercalated from $Li_{1-x}Co_{1/3}Ni_{1/3}Mn_{1/3}O_2$ and stably inserted into $Li_{1+x}Ti_5O_{12}$. Unlike metallic lithium cells, rocking chairs have no excess Li in either the anode or cathode, so they tolerate repeated discharges to 0 V.[22] Despite this robustness, the capacity decreased from 60 mAh/g to ~40 mAh/g after 50 cycles, reflecting a 36% loss of reversibility. Hence, on repeated cycling, extraction and insertion of Li ions into the structure of $LiCo_{1/3}Ni_{1/3}Mn_{1/3}O_2/Li_4Ti_5O_{12}$ was not reversible. It is difficult to fully explain this irreversibility; it is, however, evident that the $LiCo_{1/3}Ni_{1/3}Mn_{1/3}O_2$ and $Li_4Ti_5O_{12}$ cell can be used as a rechargeable cell if the capacity is improved.

Figure 2a shows the discharge curve of the all-solid-state lithium ion cell containing Li_2SiO_3 solid electrolyte between the negative and positive electrodes. Measurements of current density were performed at a constant rate of 2 nA/cm^2, a much lower rate than that used for the cell containing a liquid electrolyte. This is because of the low current available, which may have been caused by inadequate interfacial contact between the electrode and solid electrolyte. In addition, within the solid electrolyte, the available current decreased substantially because of high resistance. Please note that because of a limitation of the experimental equipment used, the applied current could not be controlled below approximately one nanoampere (<1 nA), so the discharge curve declined steeply.

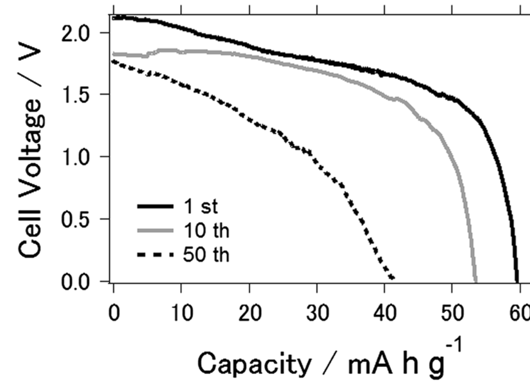

Fig. 1. Charge–discharge curve of the lithium ion cell made with $LiCo_{1/3}Ni_{1/3}Mn_{1/3}O_2$ and $Li_4Ti_5O_{12}$ containing a liquid electrolyte.

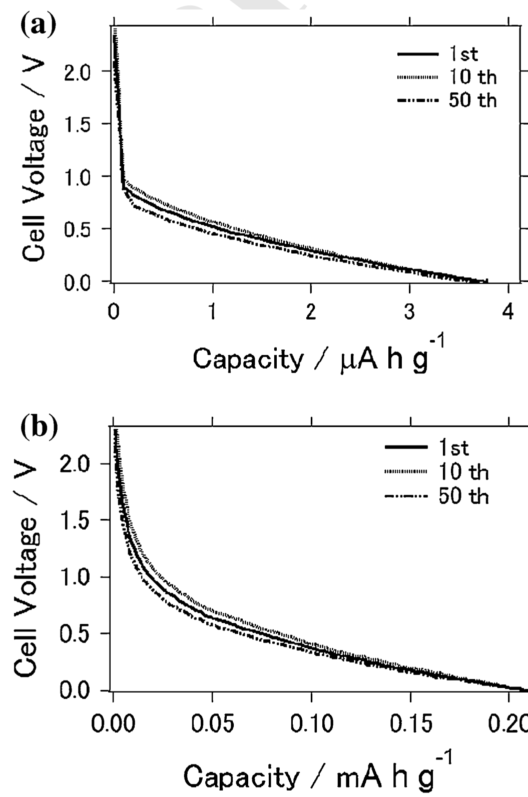

Fig. 2. Charge–discharge curve of the all-solid-state lithium ion cell. (a) Lithium ion cell composed of an $LiCo_{1/3}Ni_{1/3}Mn_{1/3}O_2/Li_2SiO_3/Li_4Ti_5O_{12}$ thin film. (b) Lithium ion cell composed of an $LiCo_{1/3}Ni_{1/3}Mn_{1/3}O_2/Li_2SiO_3/Li_4Ti_5O_{12}$ thin film with a sol–gel phase introduced into the Li_2SiO_3 layer.

This is true for Fig. 2b also. Furthermore, the measured capacitance was substantially lower than that for sulfide-based all-solid-state lithium ion cells.[10–12] We suggest that oxide particles are more rigid than sulfide particles, and this increases the resistance at particle boundaries because of the lack of particle contact to facilitate Li ion conduction. However, the capacity remained at approximately 4 μAh/g even after 50 charge–discharge cycles, indicative of the stability and strength of the all-solid-state lithium ion cell. The cell voltage was almost identical to the value obtained when the liquid electrolyte was used. Li_2SiO_3 was chosen because it was readily available for industrial use in a printable paste preparation. Although Li_4SiO_4 is a well-known lithium ion conductor, an Li_4SiO_4 solid thin film could not be prepared on $LiCo_{1/3}Ni_{1/3}Mn_{1/3}O_2$ because of film cracking.

Figure 3a is a photograph of the all-solid-state thin film lithium ion cell. The cell was prepared on a 25 mm × 35 mm aluminium board by use of a simple printing procedure. The size of the electrode and electrolyte thin films can be easily changed by modifying the squige or screen-printing methods, both of which can be readily used for industrial manufacture. Figures 3b–d show SEM images of the $Li_4Ti_5O_{12}$, Li_2SiO_3, and $LiCo_{1/3}Ni_{1/3}Mn_{1/3}O_2$

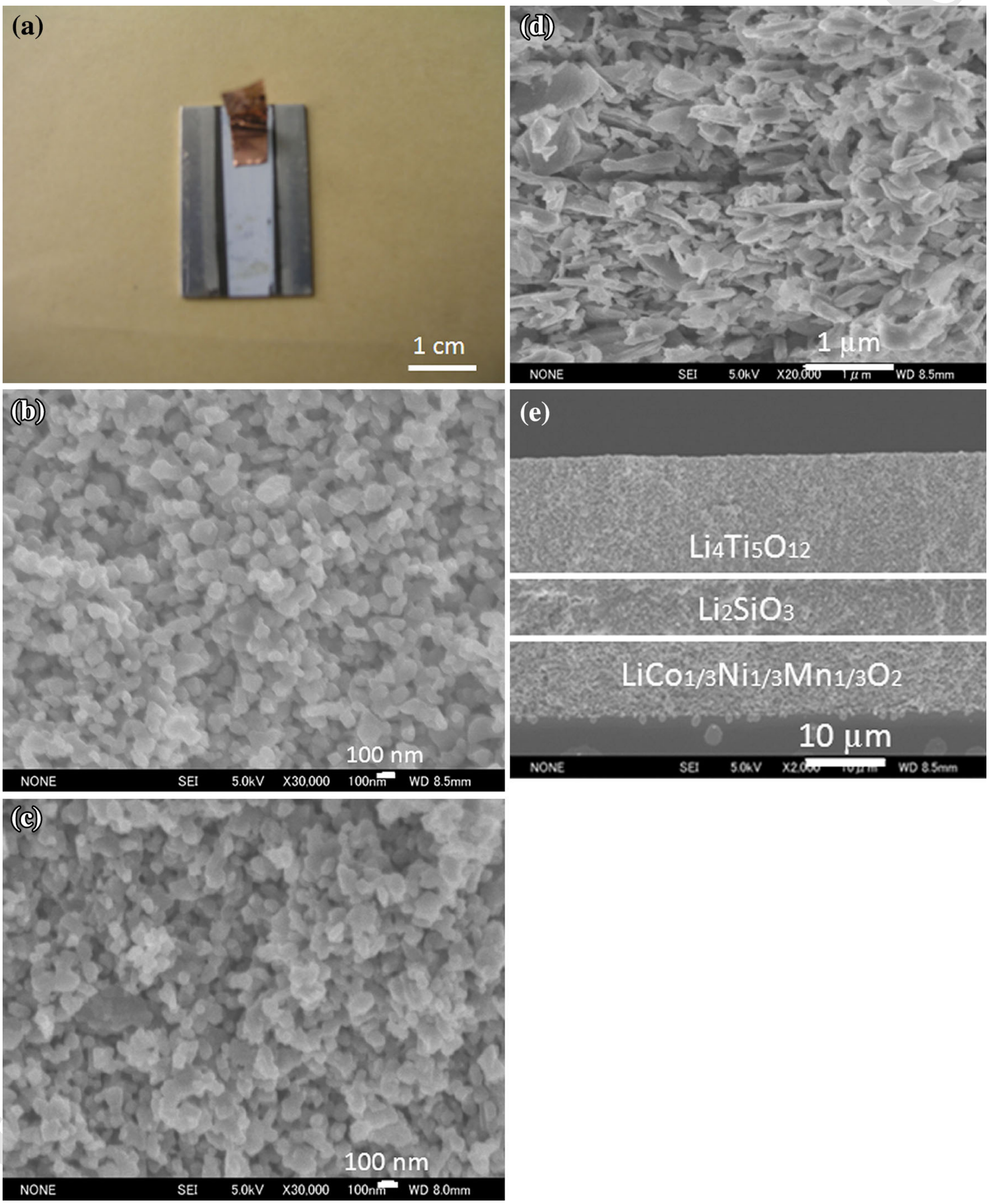

Fig. 3. (a) Photograph of the all-solid-state lithium ion cell prepared in this study. SEM image of (b) the $Li_4Ti_5O_{12}$ thin film, (c) the Li_2SiO_3 thin film, and (d) the $LiCo_{1/3}Ni_{1/3}Mn_{1/3}O_2$ thin film. (e) Cross-sectional image of $LiCo_{1/3}Ni_{1/3}Mn_{1/3}O_2/Li_2SiO_3/Li_4Ti_5O_{12}$ thin film.

Journal : 11664_JEM | Dispatch : 1-2-2014 | Pages : 8
Article No.: 3039 | ☐ LE | ☐ TYPESET
☑ CP | ☑ DISK

thin film surfaces, confirming that the particle sizes ranged between 100 nm and 200 nm for the $Li_4Ti_5O_{12}$ and Li_2SiO_3 films. Conversely, much larger (~1 μm to 2 μm) flake-like particles were observed for the $LiCo_{1/3}Ni_{1/3}Mn_{1/3}O_2$ electrode. Lu et al.[23] indicated that active material porosity in the electrode film is critical for determining cell capacitance. There should be some correlation among particle structure, size, film porosity, and film strength; these relationships require further study to enable development of better cells. Figure 3e shows the cross-sectional image of the $LiCo_{1/3}Ni_{1/3}Mn_{1/3}O_2/Li_2SiO_3/Li_4Ti_5O_{12}$ thin film. The lines that distinguish one layer from another are visible, confirming successful coating of the three layers on top of each other.

Figure 2b shows the charge–discharge curve of the cell prepared by mixing Li_2SiO_3 solid electrolyte printable paste with sol–gel solution before heat treatment. The current density was measured at a constant rate of 10 nA/cm^2. Initial capacitance was ~0.2 mAh/g and did not decrease even after 50 charge–discharge cycles, indicating that introduction of the sol–gel into the printable paste improved cell performance, including film capacitance. Our results clearly show that the solid electrolyte Li_2SiO_3 can be interchanged with liquid electrolyte to obtain the same cell voltage. Some previous studies suggest that the capacitance of lithium ion cells may be further improved by coating the surface of the active material with silica or lithium silicate.[24,25] It should be noted here that the charge–discharge experimental results obtained from the all-solid-state lithium ion cells in this study were stable to different air temperature (5–35°C) and humidity (30–70%) conditions.

Figure 4 shows an SEM image of a cross-section of an all-solid-state lithium ion cell prepared from the printable paste when sol–gel solution was added. The central region is composed of Li_2SiO_3 particles mixed with sol–gel. If this is compared with the cross-section shown in Fig. 3e, no obvious difference is apparent with regard to particle shape or size. No clear difference in the morphology was observed for the sol–gel-containing film even on inspection with SEM, and the capacity was improved. This is likely to be because the particle boundary neck was coated with solid electrolyte composed of the sol–gel phase, reducing the resistance both within the solid electrolyte and at the electrolyte/electrode interface. Liet al. et al.[24] and Mei et al.[25] have also reported that SEM did not reveal any clear differences among samples containing silica or lithium silicate, although these materials improved cell capacitance owing to enhanced Li-ion conductivity.

The Nyquist plot of the Li_2SiO_3 film prepared in this study is shown in Fig. 5. Film conductivities were estimated from the measured area and sample film thickness, which was determined from SEM cross sectional images (Figs. 3 and 4). The conductivities

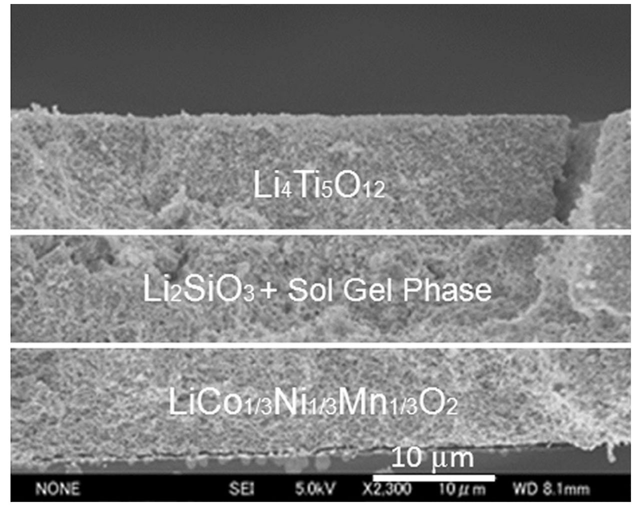

Fig. 4. Cross-sectional SEM image of all-solid-state lithium ion cell composed of an $LiCo_{1/3}Ni_{1/3}Mn_{1/3}O_2/Li_2SiO_3/Li_4Ti_5O_{12}$ thin film with a sol–gel-phase introduced into the Li_2SiO_3 layer.

were 5.56×10^{-6} S cm^{-1} for the Li_2SiO_3 film and 2.08×10^{-5} S cm^{-1} for the Li_2SiO_3 + sol–gel phase film. These are slightly higher than those obtained previously.[26] The Li_2SiO_3 film in the previous study was prepared by PLD, so the conductivity may differ because of the different method of film preparation.

Figure 6a shows the Nyquist plot for the prepared lithium ion cell. A magnified version of the Nyquist plot is also shown for the lithium ion cell containing liquid electrolyte. Figures 6b and c show the deduced electrical circuits for the lithium ion cells with liquid and solid electrolyte, respectively. For the lithium ion cell with liquid electrolyte, high and middle-range frequency was observed; this originated from the contributions of electrolyte resistance, charge-transfer resistance, and double-layer capacitance at the electrolyte/electrode interface. At low frequency the beginning of Warburg slope line is apparent; this represents the semi-infinite diffusion of Li-ions in the electrodes.[25] For the lithium ion cell with solid electrolyte, on the other hand, one large semi-circle consisting of bulk electrolyte resistance, charge transfer resistance, and double layer capacitance at the electrolyte/electrode interface was observed. Cell conductivity, estimated from measured cell area and sample film thickness, was 3.51×10^{-9} S cm^{-1} for the cell with lithium silicate solid electrolyte and 4.32×10^{-9} S cm^{-1} after introduction of sol–gel phase into the electrolyte. Comparison with the results in Fig. 5, reveals that the resistance of all the solid-state lithium ion cells prepared in this study mostly arises from the electrolyte/electrode interface and not from electrolyte film resistance. Thus, this large semi-circle is thought to arise predominantly from the charge-transfer resistance at the electrolyte/electrode interface rather than from the contribution of bulk conductivity. Nagao et al.[12] also reported that cell resistance at the electrode/electrolyte interface is

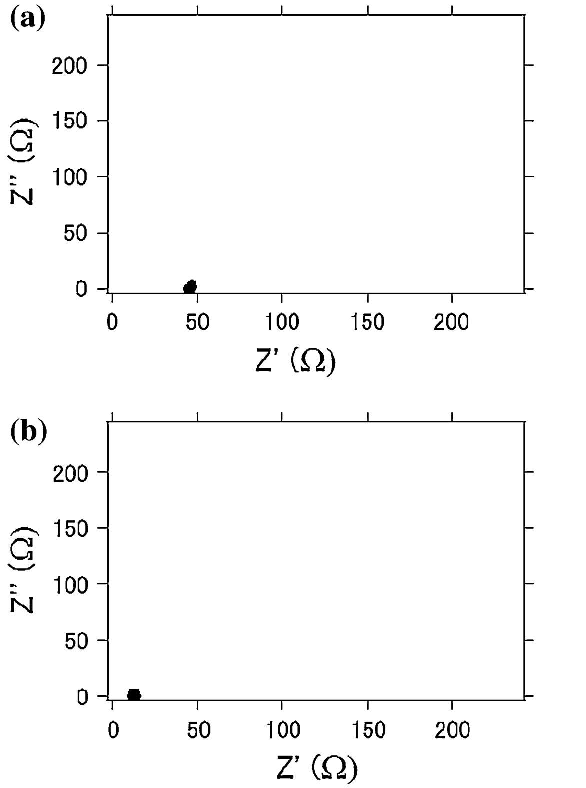

Fig. 5. Nyquist plots of Li_2SiO_3 films prepared in this study: (a) Li_2SiO_3 film; (b) Li_2SiO_3 film + sol gel phase. The insets are the cross-sectional SEM images of the measured films.

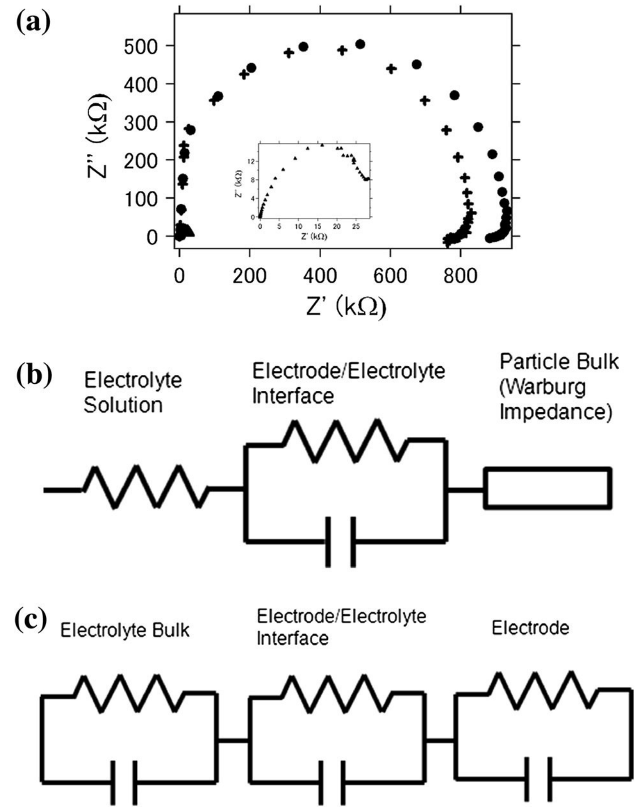

Fig. 6. (a) Nyquist plot of the lithium ion cell prepared in this study. The inset shows the Nyquist plot for the lithium ion cell containing liquid electrolyte. ▲: liquid electrolyte, ●: solid electrolyte: +: solid electrolyte and sol gel phase. (b) Equivalent electrical circuit for the lithium ion cell with liquid electrolyte. (c) Equivalent electrical circuit for the lithium ion cell with solid electrolyte.

expected to be much larger than the bulk resistance, especially for solid oxide-based electrolyte. This implies cell capacitance could be improved by optimizing the interface. As presented in Figs. 5b and 6a, although the conductivity enhancement as a result of introducing the sol–gel phase was small, the capacitance was improved. Nagao et al.[12] compared the capacitance of an all-solid-state lithium ion cell with that of a cell containing bare lithium titanate and pulverized lithium titanate; they found that although there was no clear difference between the impedance of the cells, the lithium ion cell containing pulverized lithium titanate particles had improved capacitance, owing to shortening of the Li-ion diffusion path. Similarly, it is possible that by modifying the lithium silicate solid electrolyte with sol–gel, the Li-ion diffusion path was shortened, resulting in improved cell capacitance even though the impedance and estimated conductivity were not substantially improved. Nan et al. introduced sol–gel silica into lithium lanthanum titanium oxide (LLTO) solid electrolyte and found that it enhanced ionic transport. They confirmed that lithium silicate was formed when tetraethoxysilane (TEOS) was introduced and demonstrated that lithium silicate was present mostly at grain boundaries, and not on the particle surface. In lithium ion conductive electrolytes in general, Li^+ ions are depleted at the grain boundaries owing to evaporation of Li^+ ions during the sintering process. However, Mei et al.[25] concluded that, as a result of formation of lithium silicate at grain boundaries, the Li-ion diffusion paths were formed predominantly at grain boundaries, giving rise to enhanced Li-ion conductivity. Similar results obtained by us suggest that the sol–gel phase mixed with lithium silicate was also present largely at grain boundaries and had the same effect of improving the Li ion transport.

Figure 7 shows the particle size distribution of the dispersion samples. The $D_{0.5}$ values obtained for $Li_4Ti_5O_{12}$, Li_2SiO_3, and $LiCo_{1/3}Ni_{1/3}Mn_{1/3}O_2$ were 0.76, 0.54, and 0.92 μm, respectively, which are larger than the individual particle sizes confirmed by SEM, especially for $Li_4Ti_5O_{12}$ and Li_2SiO_3. To measure the particle size, the suspension was diluted in a measurement cell, meaning that the chemical composition of the solution measured was different from that of the original solution and did not contain adequate dispersant. Therefore, some particles agglomerated, leading to the detection of larger particle sizes than were present in the original suspension. Even so, the particle size distribution for $LiCo_{1/3}Ni_{1/3}Mn_{1/3}O_2$ was larger than those observed for Li_2SiO_3 and $Li_4Ti_5O_{12}$, in reasonable agreement with the observations made by SEM.

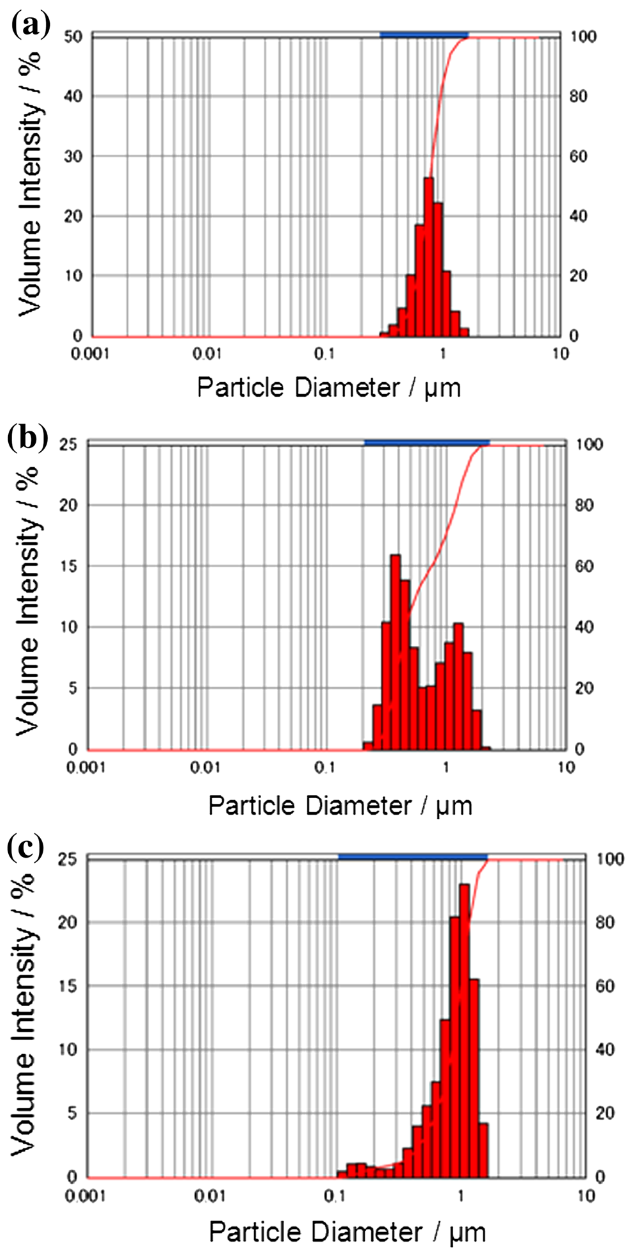

Fig. 7. Particle size distribution of the dispersion samples prepared in this study. The $D_{0.5}$ values of (a) $Li_4Ti_5O_{12}$, (b) Li_2SiO_3, and (c) $LiCo_{1/3}Ni_{1/3}Mn_{1/3}O_2$ were 0.76, 0.54, and 0.92 μm, respectively.

These results suggest that the particle dispersion method used in this study effectively controlled particle size in the prepared solid thin films. Determining the optimum particle size for all-solid-state lithium ion cells is the next step in this research.

X-ray diffraction analysis of the sol–gel phase is shown in Fig. 8. The lithium ion conductance of Li_4SiO_4–Li_3PO_4 is known to be higher than that of Li_2SiO_3.[27,28] By using a sol–gel method we attempted to prepare an Li_4SiO_4–Li_3PO_4 phase. This was expected to act as an ion-conductive inorganic glue, as explained at Fig. 5 section, within the

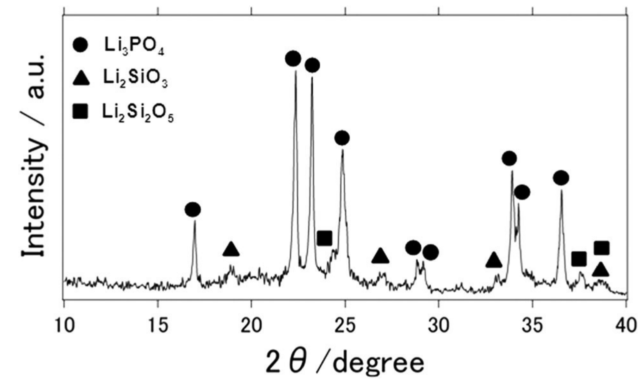

Fig. 8. X-ray diffraction pattern of the sol–gel phase prepared in this study.

solid electrolyte and at the electrode/electrolyte interface, thus reducing resistivity.[29–32] However, Li_4SiO_4 was not observed, although the Li_3PO_4 phase has the potential to be a good lithium ion conductor. Smaihi et al.[33] reported the preparation of Li_4SiO_4–Li_3PO_4 by a sol–gel method and characterized the conductivity of $Li_{4-x}Si_{1-x}P_xO_4$ at $x = 0 - 0.6$, concluding that the best conductance was obtained at $x = 0.6$. Also by using a sol–gel method, Li et al.[24] and Mei et al.[25] demonstrated that coated silica and lithium silicate were present as amorphous, not crystalline, phases. We observed that the phosphate-based crystalline phase was more dominant than the silica-based crystalline phase, even though the molar ratio of the sol–gel solution was the same as that used to prepare the Li_4SiO_4–Li_3PO_4 phase (7:1:1 = Li:Si:P). This is probably because the volatile TEOS in the sol–gel solution evaporated, causing the sintered phase to become more phosphate-rich.

However, introduction of sol–gel into the electrolyte improved the lithium ion cell capacitance. The sol–gel solution composition and preparation still require optimization to further improve cell performance. Other solid electrolytes, for example LIPON, NASICON, or LLTO are also good candidates for solid electrolytes, and can be used in this all-solid-state lithium ion cell system.

CONCLUSION

Lithium ion cell electrode material and solid electrolyte were prepared as viscous printable pastes, and films were prepared by a squige method with post-heat treatment at 600°C. It was found that the prepared thin-film electrode, used as a lithium ion-cell electrode, was stable under ambient conditions when a liquid electrolyte was used. An all-solid-state lithium ion cell composed of an $LiCo_{1/3}Ni_{1/3}Mn_{1/3}O_2/Li_2SiO_3/Li_4Ti_5O_{12}$ film structure was prepared with Li_2SiO_3 solid-electrolyte film between the cathode and anode layers. SEM observation confirmed that the three layers were lying on top of the bottom layer. The measured capacitance was

Journal : 11664_JEM Dispatch : 1-2-2014 Pages : 8
Article No.: 3039 ☐ LE ☑ CP ☐ TYPESET ☑ DISK

lower than that of a lithium ion cell with liquid electrolyte, because of the high resistance of the solid electrolyte and the electrolyte/electrode interface. We also found that cell resistance mostly arose from the electrode/electrolyte interface and not from bulk electrolyte. Cell capacitance did not decrease even after 50 charge–discharge cycles. It was also found that all-solid-state lithium ion-cell capacitance was improved by introducing a sol–gel solution into the solid electrolyte viscous printable paste. This is probably because the particle grain boundaries were coated with the sol–gel solution, reducing the resistance within the solid electrolyte and at the electrolyte/electrode interface.

ACKNOWLEDGEMENTS

The author wishes to express his thanks to Dr Sadayoshi Mori and Kazuo Sakai for helpful discussions.

REFERENCES

1. M. Hakamada and M. Mabuchi, *J. Mater. Res.* 24, 301 (2009).
2. J. Fu, *J. Am. Ceram. Soc.* 80, 1901 (1997).
3. T. Doi, Y. Iriyama, T. Abe, and Z. Qgumi, *J. Power Sources* 142, 329 (2005).
4. Y. Inaguma, C. Liquan, M. Itoh, T. Nakamura, T. Ichida, H. Ikuta, and M. Wakihara, *Solid State Commun.* 86, 689 (1993).
5. T. Abe, M. Ohtsuka, F. Sagane, Y. Iriyama, and Z. Ogumi, *J. Electrochem. Soc.* 151, A1950 (2004).
6. H. Aono, E. Sugimoto, Y. Sadaoka, N. Imanaka, and G. Adachi, *J. Electrochem. Soc.* 137, 1023 (1990).
7. R. Murugan, V. Thangadurai, and W. Weppner, *Angew. Chem. Int. Ed.* 46, 7778 (2007).
8. H. Nakano, K. Dokko, J. Sugaya, T. Yasukawa, T. Matsue, and K. Kanamura, *Electrochem. Commun.* 9, 2013 (2007).
9. M. Nakayama, S. Wada, S. Kuroki, and M. Nogami, *Energy Environ. Sci.* 3, 1995 (2010).
10. H. Kitaura, A. Hayashi, K. Tadanaga, and M. Tatsumisago, *J. Power Sources* 189, 145 (2009).
11. Y. Nishio, H. Kitaura, A. Hayashi, and M. Tatsumisago, *J. Power Sources* 189, 629 (2009).
12. M. Nagao, H. Kitaura, A. Hayashi, and M. Tatsumisago, *J. Power Sources* 189, 145 (2009).
13. A.D. Robertson, A.W. West, and A.G. Ritchie, *Solid State Ion.* 104, 1 (1997).
14. H.Y.P. Hong, *Mater. Res. Bull.* 13, 117 (1978).
15. J. Xie, N. Imanishi, T. Zhang, A. Hirano, Y. Takeda, and O. Yamamoto, *J. Power Sources* 189, 365 (2009).
16. H. Aono, H. Imanaka, and G.Y. Adachi, *Acc. Chem. Res.* 27, L78 (1994).
17. R. Mori, T. Ueta, K. Sakai, Y. Niida, Y. Koshiba, L. Lei, K. Nakamae, and Y. Ueda, *J. Mater. Sci.* 46, 1341 (2011).
18. M. Ganesan, *Ionics* 15, 609 (2009).
19. N. Kamarulzaman, R. Yusoff, N. Kamarudin, N.H. Shaari, N.A. Abdul Aziz, M.A. Bustam, N. Blagojevic, M. Elcombe, M. Blackford, M. Avdeev, and A.K. Arof, *J. Power Sources* 188, 274 (2009).
20. H. Xia, S.B. Tang, and L. Lu, *J. Alloys Compd.* 449, 296 (2008).
21. Y.J. Shin, W.J. Choi, Y.S. Hong, S. Yoon, K.S. Ryu, and S.H. Chang, *Solid State Ion.* 177, 515 (2006).
22. M. Manicham and M. Takata, *J. Power Sources* 114, 298 (2003).
23. W. Lu, A. Jansen, D. Dees, and G. Henriksen, *J. Mater. Res.* 25, 1656 (2010).
24. Y. Li, S. Zhao, C. Nan, and B. Li, *J. Alloy Compd.* 509, 957 (2011).
25. A. Mei, X.L. Wang, Y.C. Feng, S.J. Zhao, G.J. Li, H.X. Geng, Y.H. Lin, and C.W. Nan, *Solid State Ion.* 179, 2255 (2008).
26. A. Nakagawa, N. Kuwata, Y. Matsuda, and J. Kawamura, *J. Phys. Soc. Jpn.* 79, 98 (2010).
27. R.D. Shannon, B.E. Taylor, A.D. English, and T. Berzins, *Electrochim. Acta* 22, 783 (1977).
28. Y.-W. Hu, I.D. Raistrick, and R.A. Huggins, *J. Electrochem. Soc.* 124, 1240 (1997).
29. A. Sakuda, H. Kitaura, A. Hayashi, K. Tadanaga, and M. Tatsumisago, *Electrochem. Solid-State Lett.* 11, A1 (2008).
30. A. Sakuda, H. Kitaura, A. Hayashi, K. Tadanaga, and M. Tatsumisago, *J. Electrochem. Soc.* 156, A27 (2009).
31. A. Sakuda, H. Kitaura, A. Hayashi, K. Tadanaga, and M. Tatsumisago, *J. Power Sources* 189, 527 (2009).
32. Y. Sakurai, A. Sakuda, H. Kitaura, A. Hayashi, and M. Tatsumisago, *Solid State Ion.* 182, 59 (2011).
33. M. Smaihi, D. Petit, F. Gourbilleau, F. Chaput, and J.P. Boilot, *Solid State Ion.* 48, 213 (1991).

Journal : 11664_JEM | Dispatch : 1-2-2014 | Pages : 8
Article No.: 3039 | ☐ LE ☑ CP | ☐ TYPESET ☑ DISK